THE JOURNAL OF PHYSICAL CHEMISTRY B LETTERS

2005, *109,* 8533−8537
Published on Web 04/12/2005

Hidden Minima of the Gibbs Free Energy Revealed in a Phase Separation in Polymer/Surfactant/Water Mixture

R. Hołyst,*,†,‡ K. Staniszewski,† A. Patkowski,§ and J. Gapiński§

Institute of Physical Chemistry, Polish Academy of Sciences, Department III, Kasprzaka 44/52, 01224 Warsaw, Poland, Department of Mathematics and Natural Sciences, College of Science, Cardinal Stefan Wyszyński University, Dewajtis 5, 01-815 Warsaw, Poland, and Department of Physics, A. Mickiewicz University, Umultowska 85 61-614 Poznań, Poland

Received: February 4, 2005; In Final Form: March 24, 2005

We observed a very unusual kinetic pathway in a separating $C_{12}E_6$/PEG/H_2O ternary mixture. We let the mixture separate above the spinodal temperature (cloud point temperature) for some time and next cool it into a metastable region of a phase diagram, characterized by two minima of the Gibbs potential, one corresponding to the homogeneous mixture and one to the fully separated PEG-rich and $C_{12}E_6$-rich phases. Despite the fact that in the metastable region the thermodynamic equilibrium corresponds to the separated phases (global minimum of the Gibbs free energy), we observe perfect mixing of the initially separated phase. The homogeneous state, obtained in this way, does not separate, if left undisturbed. However, many cooling−heating cycles or full separation with visible meniscus above the cloud point temperature induce the phase separation in the metastable region. The metastable region can exist tens of degrees below the cloud point temperature. This effect is not observed in the binary mixture of $C_{12}E_6$/H_2O.

A phase diagram for a binary mixture can be divided into three regions: the one-phase region, where the only minimum of the Gibbs free energy corresponds to the uniform (homogeneous) state, the metastable region, where the global (the deepest) minimum of the free energy corresponds to the separated phases, but the local minimum corresponds to the homogeneous mixture, and finally the unstable (spinodal region), where the only minimum of the free energy corresponds to the separated phases. In the latter case the homogeneous mixture is unstable with respect to any small changes of concentrations, whereas in the metastable region, there is an energy barrier for the phase separation.

The kinetic pathway, which is usually studied in the phase separation process, is the transformation of the initially homogeneous state to a nonuniform (phase separated) state and its further coarsening in time.[1,2] When a homogeneous *A*/*B* mixture (say surfactant/water mixture) below its upper critical point is suddenly heated above its critical temperature, it ceases to be in the thermodynamical equilibrium and starts to separate. The homogeneous state can now be either a metastable or an unstable state. In the former case, the process of demixing requires, in the first place, nucleation of droplets of a minority phase, say *A*-rich phase. Then the droplets start to grow. When the system is quenched into the thermodynamically unstable region, the demixing proceeds via the spinodal decomposition mechanism; that is, the system becomes unstable with respect to infinitesimaly small fluctuations of concentrations. In the metastable region, we have to wait for the separation process for a time needed to overcome the nucleation energy barrier via large fluctuation, while in the unstable region the demixing is instanteneous.

The reverse process to the one described above of a decay of the nonuniform configurations into the homogeneous one has recently received more attention.[3−6] In ref 3, the fully separated binary mixture, with upper consolute (critical) point, was heated to the one-phase region and the processes of mixing was observed. It revealed unusually large fluctuations in composition, orders of magnitude larger than at equilibrium. It was also shown[4−6] that when a partially separated mixture (many domains of one phase in the matrix of another phase) is quenched into the metastable region the domains partially dissolve and afterward start to grow again. The dissolution of the domains in the homogeneous phase is of course complete.

It is the purpose of this paper to show that the phase behavior can be much more complicated than the commonly accepted scenario. One of the issues not well understood is the energy landscape of the Gibbs free energy, which is responsible for different kinetic pathways in phase separation processes. The following question can be posed: Can we completely mix a phase-separated system in the metastable region? The answer depends on the Gibbs energy landscape. In Figure 1, we show one possible scenario where after a separation in the unstable region we can obtain a perfect mixing in the metastable region. Figure 1 shows a cartoon representation of the energy landscape of the Gibbs free energy in the one-phase, metastable, and unstable regions with two minima in the metastable state, one corresponding to the homogeneous mixture and one to the separated phases. If the minimum corresponding to the homogeneous mixture is very wide and shallow, the system may stay very long in this minimum before crossing the barrier and going

* To whom correspondence should be addressed.
† Polish Academy of Sciences.
‡ Cardinal Stefan Wyszyński University.
§ A. Mickiewicz University.

10.1021/jp050634y CCC: $30.25

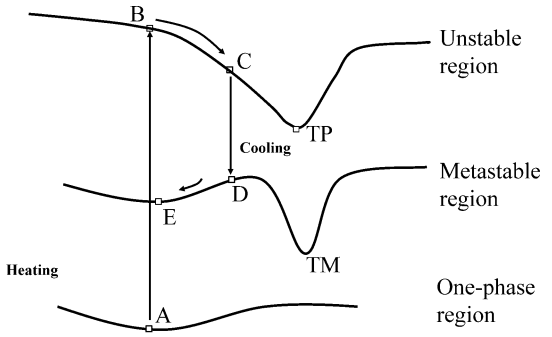

Figure 1. Cartoon representation of a probable kinetic pathway observed in our experiment, with a sketch of the Gibbs free energy in the homogeneous, metastable, and unstable regions of a phase diagram as a function of the concentration in one of the phases. Point A is the equilibrium state of the homogeneous mixture, and point E represents the metastable state for the homogeneous mixture. Points TP and TM represent the minima corresponding to the fully separated mixture (see text for more details). In general, the Gibbs free energy is a functional of the concentration distribution in the system and should be represented approximately in the multidimensional space of concentrations; that is, for each point **r** in the system, we specify a concentration $c(\mathbf{r})$ of the components and they together form a space where the Gibbs landscape can be drawn.

into the separated configuration. Such a landscape is characteristic for systems with low surface tensions, i.e., containing surfactants. We applied optical microscopy, static light scattering, photon correlation spectroscopy,[7] and macroscopic observations in thick capillaries to study separation/mixing processes in the ternary mixture of surfactant, polymer, and water system. The cartoon shown in Figure 1 grasps the idea of the observations made. The system is prepared in the one-phase region of a phase diagram where the Gibbs potential has only one minimum corresponding to the homogeneous phase (point A Figure 1). In the metastable region, there are two minima (E,TM), where the second one (TM) corresponds to the separated phases. Finally, in the unstable region, there is only one minimum (TP) corresponding to the separated phases. First we heat the sample (line A−B) into the unstable region and observe how the separation process proceeds (B−C). We stop the separation at point C before reaching the second minimum (point TP) and cool the mixture into the metastable region (line C−D) and observe the homogenization process (line D−E); that is, the system comes back to the local minimum corresponding to the homogeneous phase (point E Figure 1). Such behavior is however unusual and has not been observed so far. In the experiment, we can run the phase separation for 40−60 min and obtain 10−100 μm size domains of one of the phases and still be able to homogenize the mixture in the metastable region. It is only when the separation is complete (two phases with a flat interface between them) (point TP) that we cannot homogenize the mixture by lowering the temperature into the metastable region as is evident from the cartoon. Interestingly, we can keep the homogeneous mixture in the metastable state for weeks without inducing the transition (phase separation) to the global minimum of the Gibbs potential. In this sense, it is a hidden global minimum.

We used the nonionic surfactant $C_{12}E_6$ (hexaethylene glycol monododecyl ether) purchased from Fluka of purity better than 98%. The melting temperature given by Fluka Chemical Co. for pure $C_{12}E_6$ was between 27 and 28 °C, and our measurement using differential scanning calorimetry gave 27.11 °C. The molecular weight of the surfactant is 450.66. The polymer PEG (poly(ethylene glycol)) was purchased from Merck. The molecular mass of PEG was 6000, 8000, and 20 000. Water was distilled, filtered with the Millipore filters, and degassed. The mixtures were prepared at room temperature in a humid atmosphere in order to avoid evaporation of water. From the prepared mixture, we have made thin samples in the following way: First a drop of solution was placed on a glass plate (cleaned in ultrasound cleaner). Next it was covered by the second glass plate. To control the thickness, we have placed the copper wire spacer of known thickness (12 μm) between two glass plates. Finally, the samples were sealed with an epoxy resin glue in order to avoid the evaporation of water during the measurements. These samples were used for the optical microscopy measurements. Optical microscopy measurements were performed using the Nikon Eclipse E 400 microscope with crossed polarizers, equipped with the heating/cooling stage LINKAM THMS 600. The temperature was controlled up to 0.01 °C and the sudden jump in temperature (10−30 °C) took only 30 s.

The photon correlation spectroscopy experiments were carried out using a Zeiss Helium−Neon laser HNA 188-S (former East Germany), operated at $\lambda = 632.8$ nm delivering up to 50 mW of linearly polarized light. The scattered light was collected using a mono-mode optical fiber mounted on the arm of a goniometer (ALV/SP-125, ALV GmbH, Langen, Germany) and fed into a high quantum efficiency photon counting avalanche photodiode (APD unit, ALV GmbH, Langen, Germany). The useful range of the scattering angle θ was 30°−150°, resulting in the accessible range of the scattering vector magnitude q between 6.836×10^6 and 2.551×10^7 m^{-1} ($q = 4\pi n/\lambda \sin(\theta/2)$, where the refractive index of water $n = 1.33$). The sample was filtered (0.2 μm Millipore disposable filter units) directly into a cylindrical 10 mm diameter glass cell. Before measurements, the cell with the sample was centrifuged for 20 min at 8000 g to remove air bubbles. During the light scattering measurements, the temperature of the sample holder was maintained with an accuracy of 0.1 °C. A digital correlator ALV5000E (ALV GmbH, Langen, Germany) was used to calculate the autocorrelation function of scattered light intensity with the resolution of $\Delta t = 200$ ns, allowing measurements of the relaxation times in the range 10^{-5}−1000 s. The diffusion coefficients were calculated from the q^2 dependence of the fitted relaxation time ($1/\tau = Dq^2$).

In Figure 2, we show the phase diagram for the ternary mixture of surfactant−water mixture with the addition of PEG. Each curve represents the cloud point measurements (obtained in optical study and in static light scattering experiments). The samples were heated to the temperature where the mixture became turbid instanteneously indicating phase separation. The scattering of light was thus clearly visible. Above each curve, the homogeneous mixture is unstable with respect to separation. Below each curve, the thermodynamic state of the mixture is either metastable or homogeneous. We could keep the homogeneous mixture below these curves for weeks without observing any phase separation. Moreover, when we induced separation in thin samples and next cooled it down below this curve, a perfect mixing occurred, and the samples returned to the homogeneous state.

In Figure 3, we show separation/mixing processes in thin samples (12 μm) of 10% $C_{12}E_6$, 7% PEG (6000), and water obtained from the optical microscope observations. In Figure 3a, we show an image of a sample below the cloud curve shown in Figure 2 at 25 °C heated slowly from 20 °C. We heated the sample to 30 °C and induced a phase separation process shown in Figure 3b (image obtained after 40 min of separation). Next

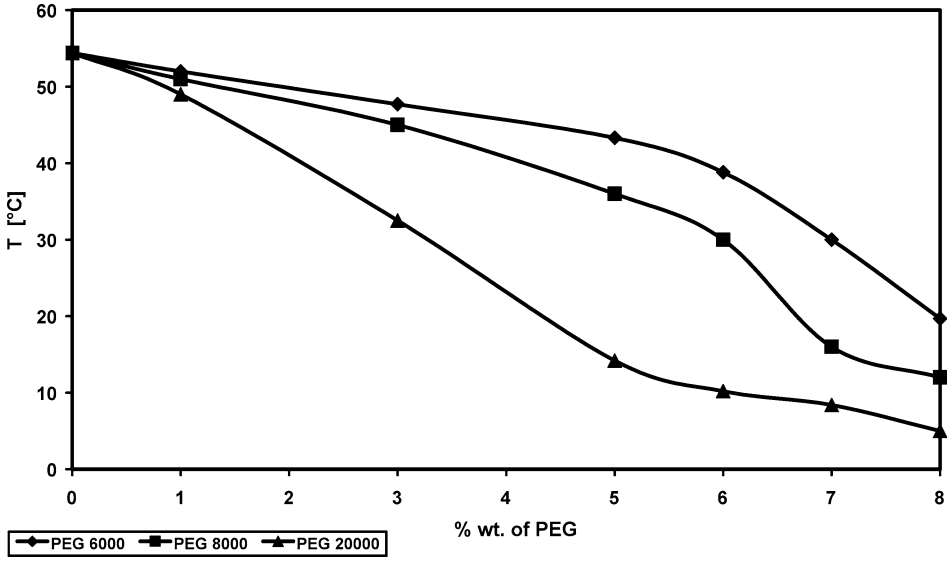

Figure 2. Temperature versus the weight fraction of PEG (with respect to water) for the mixture of 10% $C_{12}E_6$/PEG/water. The lines (to guide the eyes) show the cloud point measurements, i.e., determine the line dividing metastable and unstable region in the phase diagram. The separation process starts on the line immediately after the temperature jump (triangles are for PEG 20000, squares for PEG 8000, and diamonds for PEG 6000). Below these lines the mixture does not separate for weeks if left undisturbed. However, in the experiment with many heating−cooling cycles, we can also induce separation even tens of degrees below the lines.

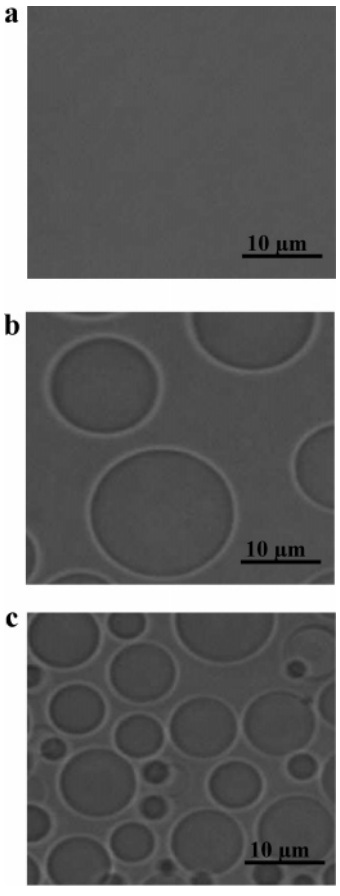

Figure 3. Images from the optical microscope in thin samples of 12 μm thickness. (a) Homogeneous phase at 25 °C after a temperature jump from 20 °C. (b) Phase separation process 40 min after the temperature jump from 20 to 30 °C. (c) Phase separation process at 25 °C after 10 heating−cooling cycles between 20 and 30 °C. Interestingly, if after the first cycle we cool the system from 30 °C (Figure 3b) during the phase separation to 25 °C, the domains shown in (b) disappear and the sample becomes homogeneous as shown in (a).

we cooled the sample back to 25 °C and got perfect mixing; that is, we obtained the same image as shown in Figure 3a.

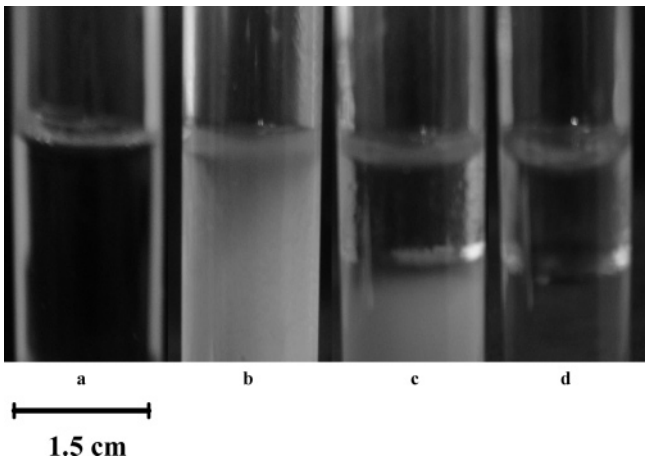

Figure 4. Photographs of the samples in thick capillaries. (a) Homogeneous phase at 25 °C. (b) Turbid sample at 30 °C. (c) Fully separated sample with visible air-phase I meniscus and phase I−phase II meniscus at 30 °C. (d) Fully separated sample with a clear second meniscus between two phases at 25 °C, after being cooled from (c). When we cooled a turbid sample (b) before completion of the phase separation to 25 °C, we obtained (a) i.e., homogeneous sample.

Next we performed 10 heating/cooling cycles (between 20 and 30 °C) and eventually separated the mixture at 25 °C (shown in Figure 3c after 10 min of the separation). This is a direct proof that at 25 °C the system is metastable since eventually we were able to induce phase separation at this temperature. However, the sample never separates at this temperature if left undisturbed.

In Figure 4, we show the same scenario in a thick capillary in order to prove that mixing and unusual kinetics is not due to the surface effects (under the microscope we observed thin samples of 12 μm size). In Figure 4a, a homogeneous mixture (same composition as in Figure 3) is shown at 25 °C. In Figure 4b, the sample was heated to 30 °C, and the sample became turbid indicating phase separation. When cooled back to 25 °C, the sample mixed again (same image as in Figure 4a). However, if we allowed the mixture to achieve a fully separated state with a visible meniscus separating the two phases (Figure 4c) and

cooled it back to 25 °C, the sample stayed in the separated state as shown in Figure 4d. No further mixing was observed at this temperature. This experiment supports the cartoon scenario shown in Figure 1; that is, if the separation process brings the mixture to its final fully separated state (global minimum of the Gibbs free energy), the mixture cannot come back into the homogeneous state (local minimum of the Gibbs free energy) after cooling.

The optical observation does not tell us much about the local structure in the mixture. Even if the mixture is transparent and not turbid, we cannot tell if the homogeneous state obtained after cooling the sample from the unstable region is the same as the homogeneous state obtained for fresh samples. In dynamic light scattering experiments, we are able to determine the relaxation processes (fluctuations of the concentration) which usually very strongly depend on the microscopic structure of the system. In the photon correlation spectroscopy, we measure the intensity−intensity correlation function of the scattered light

$$F(q, t) = \langle I(q, 0)I(q, t)\rangle \tag{1}$$

as a function of time, t, and the scattering wavevector, $q \neq 0$. Assuming that the average in eq 1 is over the Gaussian distribution, we can rewrite $F(q, t)$ in the following form:

$$F(q, t) = \langle I(q, 0)\rangle\langle I(q, 0)\rangle(1 + \beta C(q, t)^2) \tag{2}$$

where $C(q, t)$ is the autocorrelation function and $0 < \beta < 1$ is the factor, which depends on the experimental setup. In the homogeneous phase, $\langle I(q, t)\rangle = \langle I(q, 0)\rangle$ is independent of time. The relaxation of the concentration fluctuations have the following form:

$$C(q, t) = \sum_i A_i \exp(-t/\tau_i) \tag{3}$$

where i numbers different relaxation processes in the mixture and τ_i is a characteristic time over which this relaxation process occurs. If the relaxation process is driven by pure diffusion, as observed in our ternary mixture, we have

$$\tau_i = \frac{1}{D_i q^2} \tag{4}$$

where D_i is the collective translational diffusion coefficient. We have determined D_i in binary PEG/water and $C_{12}E_6$/water mixtures and in ternary $C_{12}E_6$/PEG/water mixtures in homogeneous samples and in separated phases. In the binary mixtures, the auto-correlation function (eq 3) was monoexponential characterized by a single collective diffusion coefficient D. For example, $D = 3.7 \times 10^{-7}$ cm^2/s for the 10% $C_{12}E_6$/water system at 18 °C. In the binary PEG/water system, $D = 5 \times 10^{-7}$ cm^2/s for a 1% solution of PEG 20 000 and $D = 8 \times 10^{-7}$ cm^2/s for a 1% solution of PEG 6000 at 18 °C. Interestingly D increased with the PEG concentration to $D = 9.5 \times 10^{-7}$ cm^2/s for 7% solution of PEG 20000 and $D = 1.2 \times 10^{-6}$ cm^2/s for 7% solution of PEG 6000 at 18 °C. In homogeneous ternary mixtures $C(q, t)$ could be fitted with a single exponential, and the signal was dominated by scattering from either surfactant micelles or aggregates (scattering from PEG is very weak). The collected data of D in the homogeneous phase are shown in Figure 5 for PEG 6000. By inducing separation at temperatures below the cloud curve (Figure 2), we could measure the diffusion coefficients in the separated phases. In separated phases, there were two components and $C(q, t)$ could be fitted with two exponentials. In all cases studied, the collective

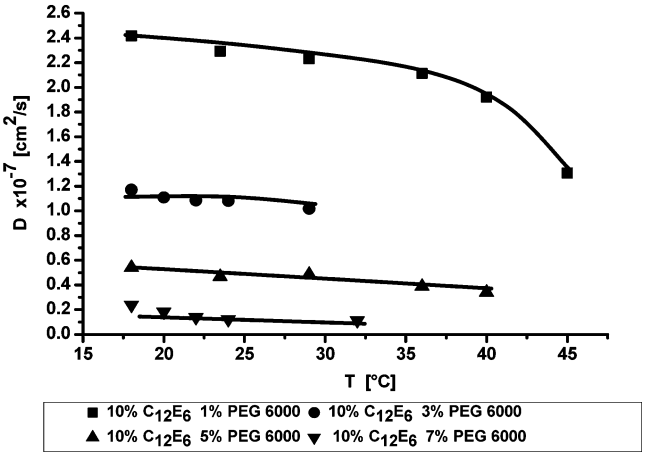

Figure 5. Collective translational diffusion coefficient measured by the photon correlation spectroscopy as a function of temperature for four different mixture 10% $C_{12}E_6$/1%, 3%, 5%, 7% PEG 6000/water in the homogeneous phase. Lines are added to guide the eyes. The collective translational diffusion in the homogeneous state (or hidden metastable state) is many times smaller than the collective diffusion coefficients in the separated phases (given in the main body of the paper). Similar measurements were done for PEG 8000 and PEG 20000.

diffusion coefficient was the same for a fresh sample and for the homogeneous sample obtained after initial separation and further cooling. It means that in all cases the mixing process was complete and did not depend on the history of the sample. Interestingly, in the separated phases, the collective diffusion coefficients were at least a few times larger than in the homogeneous phase. For example (Figure 5) at 18 °C, $D = 2.4 \times 10^{-8}$ cm^2/s in the homogeneous phase consisting of 10% of $C_{12}E_6$ and 7% of PEG 6000, whereas after separation at this temperature, we found that in the upper phase (see Figure 4) $D_1 = 1.1 \times 10^{-6}$ cm^2/s and $D_2 = 4.7 \times 10^{-8}$ cm^2/s and in the lower phase (Figure 4) $D_1 = 1.1 \times 10^{-6}$ cm^2/s and $D_2 = 1.4 \times 10^{-7}$ cm^2/s. The same general trend was found for PEG 8000 and PEG 20000. Thus, because the diffusion coefficient in r the homogeneous phase is the same irrespective of the thermal history of the sample, we conclude that the homogenization process was complete and the structure of the homogeneous phase was the same in the fresh sample and in the sample which was first separated at high temperature before remixing. Although the mixtures of PEG/surfactant and water were studied previously by the photon correlation spectroscopy, the collective diffusion coefficients in separated phases and the metastable effects have not been determined.[8−10]

Finally, we note that the metastable region can be very wide. For example, the cloud point measurements (Figure 2) for the ternary mixture consisting of 10% of $C_{12}E_6$ and 7% of PEG 6000 gave a temperature of separation of 30 °C, whereas we have been able to separate the sample at 18 °C. In a mixture of 10% of $C_{12}E_6$ and 1% of PEG 8000, the cloud point measurements gave 50 °C, but we could separate the mixture at 18 °C. We could not determine the exact temperature where the metastability still persisted. Normally, we could homogenize all samples (Figure 2) at 4 °C. Metastability was not observed for binary PEG/water or surfactant/water mixtures.

In conclusion, the kinetic pathways in phase transitions depend on the Gibbs free energy landscape (Figure 1). In the presented system (surfactant/polymer/water ternary mixture), some of the minima of the Gibbs potential (global minimum in the metastable region) could not be easily revealed. In particular, we have shown that the metastable thermodynamic state can

be very easily taken for the stable equilibrium thermodynamic state for the homogeneous mixture.

Acknowledgment. This work has been supported by the KBN Grant 3T09A09727 (2004-2007).

References and Notes

(1) Bray, A. J. *Adv. Phys*. **1994**, *43*, 357.

(2) Langer, J. S. In *Solids far from Equilibrium*; Godreche, C., Ed.; Cambridge University Press: New York, 1992; p 297.

(3) Vailati, A.; Giglio, M. *Nature* **1997**, *390*, 262. Vailati, A.; Giglio, M. *Phys. Rev. E* **1998**, *58*, 4361. Ciecuta, P.; Vailati, A.; Giglio, M. *Phys. Rev. E* **2000**, *62*, 4920.

(4) Graca, M.; Wieczorek, S. A.; Fialkowski, M.; Hołyst, R. *Macromolecules* **2002**, *35*, 9117.

(5) Graca, M.; Wieczorek, S. A.; Hołyst, R. *Macromolecule*s **2002**, *35*, 7718.

(6) Fialkowski, M.; Hołyst, R. *J. Chem. Phys.* **2002**, *117*, 1886; **2004**, *120*, 5802.

(7) Berne, B. J.; Pecora, R. *Dynamic Light Scattering with Applications to Biology, Chemistry and Physics*; Wiley-Interscience: New York, 1976.

(8) Feitosa, E.; Brown, W.; Vasilescu, M.; Swanson-Vethamuthu, M. *Macromolecules* **1996**, *29*, 6837.

(9) Feitosa, E.; Brown, W.; Wang, K.; Barreleiro, P. C. A. *Macromolecules* **2002**, *35*, 201.

(10) Feitosa, E.; Brown, W.; Swanson-Vethamuthu, M. *Langmuir* **1996**, *12*, 5985.